Published in final edited form as:
Nat Commun. 2014 ; 5: 3200. doi:10.1038/ncomms4200.

Integration of molecular and enzymatic catalysts on graphene for biomimetic generation of antithrombotic species

Teng Xue[1,*], **Bo Peng**[2,*], **Min Xue**[3], **Xing Zhong**[3], **Chin-Yi Chiu**[1], **Si Yang**[2], **Yongquan Qu**[3], **Lingyan Ruan**[1], **Shan Jiang**[3], **Sergey Dubin**[3], **Richard B. Kaner**[1,3,4], **Jeffrey I. Zink**[3,4], **Mark E. Meyerhoff**[2], **Xiangfeng Duan**[3,4], and **Yu Huang**[1,4]

[1]Department of Materials Science and Engineering, University of California, Los Angeles, California 90095, USA

[2]Department of Chemistry, The University of Michigan, 930 N. University, Ann Arbor, Michigan 48109, USA

[3]Department of Chemistry and Biochemistry, University of California, Los Angeles, California 90095, USA

[4]California NanoSystems Institute, University of California, Los Angeles, California 90095, USA

Abstract

The integration of multiple synergistic catalytic systems can enable the creation of biocompatible enzymatic mimics for cascading reactions under physiologically relevant conditions. Here we report the design of a graphene–haemin–glucose oxidase conjugate as a tandem catalyst, in which graphene functions as a unique support to integrate molecular catalyst haemin and enzymatic catalyst glucose oxidase for biomimetic generation of antithrombotic species. Monomeric haemin can be conjugated with graphene through π–π interactions to function as an effective catalyst for the oxidation of endogenous L-arginine by hydrogen peroxide. Furthermore, glucose oxidase can be covalently linked onto graphene for local generation of hydrogen peroxide through the oxidation of blood glucose. Thus, the integrated graphene–haemin–glucose oxidase catalysts can readily enable the continuous generation of nitroxyl, an antithrombotic species, from physiologically abundant glucose and L-arginine. Finally, we demonstrate that the conjugates can

Correspondence and requests for materials should be addressed to M.E.M. (mmeyerho@umich.edu) or to X.D. (xduan@chem.ucla.edu) or to Y.H. (yhuang@seas.ucla.edu).
*These authors contributed equally to this work.

Author contributions
Y.H., X.D. and M.E.M. designed the research. T.X. and B.P. performed most of the experiments and data analysis. M.X. contributed to the DAF assay. X.Z., C.-Y.C. and Y.Q. contributed to the characterization of catalyst conjugates. S.Y. contributed to the chemiluminescence experiments. L.R. conducted zeta potential analysis. S.J. and S.D. contributed to catalyst conjugate synthesis. R.B.K., J.I.Z., M.E.M., X.D. and Y.H. supervised the research. T.X., X.D., M.E.M. and Y.H. co-wrote the paper. All authors discussed the results and commented on the manuscript.

Additional information
Supplementary Information accompanies this paper at http://www.nature.com/naturecommunications

Competing financial interests: The authors declare no competing financial interests.

Reprints and permission information is available at http://npg.nature.com/reprintsandpermissions/

be embedded within polyurethane to create a long-lasting antithrombotic coating for blood-contacting biomedical devices.

Biological systems can often drive complex chemical transformations under mild conditions (for example, aqueous solution, physiological pH, room temperature and atmospheric pressure), which is difficult to achieve in conventional chemical reactions. This unique ability is generally empowered by a series of synergistic protein catalysts that can facilitate reaction cascades through complex metabolic pathways. There is significant interest in exploring molecular assemblies and/or conjugated catalytic systems as analogues to the functional proteins that can facilitate chemical transformations under biologically mild conditions[1]. Although 'artificial enzymes' have been studied for decades[2], catalysts mimicking true enzymes for designated and complex reaction pathway have been much less frequently explored. The integration of enzymatic catalysts with molecular catalysts could create functional tandem catalytic systems for important chemical transformations not otherwise readily possible[3,4]. Despite the significant interest[5–7], it is quite challenging to build a system that can allow enzymatic catalysts and molecular catalysts to operate synergistically under the same conditions (for example, aqueous solutions and physiological pH).

Conjugation of these two distinct catalyst systems on a common platform support offers a plausible pathway. In this regard, the single-atom layer thick material graphene represents an interesting support for both enzymatic and molecular catalysts owing to several of its unique characteristics. First, bulk quantities of graphene flakes can now be readily prepared through chemical exfoliation of graphite oxide (GO) followed by chemical reduction[8–13]. Chemically reduced graphene typically possesses a large number of functional groups at the edges or defect sites to enable solubility/dispersibility in various solvents. These functional groups can also allow flexible covalent chemistry for linkage with molecular systems or enzymes. In addition, the extended π surface of graphene can also enable further functionalization via cation–π or π–π interactions. This rich surface chemistry offers excellent potential for coupling multiple distinct catalysts on graphene to create tandem catalysts for reaction cascading. Furthermore, the two-dimensional structure of graphene provides a unique geometry as a catalyst support with a large open surface area that is readily accessible to substrates/products with minimal diffusion barriers. Finally, it has been shown that graphene has better biocompatibility than other carbon nanomaterials for potential biomedical applications[14].

Thrombus formation is one of the most common and severe problems that lead to complications of blood-contacting biomedical devices including catheters, vascular grafts and heart valves[15]. Therefore, it is of considerable interest to develop an antithrombotic coating on biomedical devices that can sustain their functionality, decrease failure rate, and therefore greatly reduce associated medical complications and cost. Nitric oxide (NO) is recognized as a potent antiplatelet agent that can help prevent thrombus formation[16]. The extraordinary thrombo-resistant nature of healthy blood vessels is largely attributed to the continuous production of low fluxes (*ca.* 0.5~4.0 × 10^{-10} mol cm^{-2} min^{-1}) of NO by the endothelial cells that line the inner walls of all blood vessels[17]. The design and fabrication of

polymeric coatings capable of releasing or generating NO has recently drawn considerable attention for mitigating the risk of thrombus formation. A significant portion of the studies have focused on exogenous NO donors such as diazeniumdiolates[18], which can immediately release NO when exposed to water or physiological environments (that is, blood, body fluids and so on). Such artificial polymeric coatings with embedded or covalently linked NO donors release NO to minimize thrombus formation[19–21]. However, the application of this approach for long-term implants, such as vascular grafts or haemodialysis catheters, is limited by the inevitable depletion of the finite reservoir of reagents in an exogenous NO donor source[22]. In addition, the labile nature of most NO donors (heat, light and moisture sensitivity) curtails their practical manufacturability and clinical applications. Moreover, the toxicity of some diazeniumdiolate precursors and the potential formation of carcinogenic nitrosamine by-products may also pose an adverse effect[23]. Alternatively, a surface coating capable of catalytic generation of NO from physiological components may offer a more attractive strategy for sustained NO release. For example, organoselenium[24,25] has been shown to trigger the decomposition of *S*-nitrosothiols, well-known endogenous NO carriers, to generate NO; this strategy is potentially useful for the continuous release of NO over long time periods. However, the relatively low level and highly variable concentrations of endogenous nitrosothiols in blood[26] limit the reliability of these NO-generating materials. *In vivo* toxicity studies also suggested that the reaction between reduced selenium species and oxygen is fast enough to produce a significant amount of superoxide that can react with NO to produce peroxynitrite, a toxic species[27]. In addition, selenium radical formation is also problematic, although aromatic organoselenium species have been found to be far less toxic (for example, ebselen[28]).

Biologically, NO is believed to arise from the oxidation of L-arginine catalysed by a family of nitric oxide synthase enzymes that utilize the reduced form of nicotinamide adenine dinucleotide phosphate (NADPH) as a cofactor along with O_2 as the oxidant[29,30]. Under conditions where the L-arginine concentration and/or cofactor supplies are limited, nitroxyl (HNO), the one electron reduced form of NO, can also be produced[31]. HNO has been studied extensively with regard to its provocative and pharmacological importance for heart failure treatment[31], and it has recently been reported that HNO possesses antithrombotic activity analogous to NO[32]. Previous studies also indicate that hydrogen peroxide can substitute for NADPH and O_2 as the oxidant for HNO production[33,34]. Thus, biomimetic generation of antithrombotic HNO is a possible solution to the problems associated with NO-releasing materials and NO-generating catalysts. However, to date, there is no report of a biocompatible surface capable of local generation of HNO for effectively minimizing thrombus formation. Here we report a new design of graphene–haemin–glucose oxidase (GOx) conjugate as a tandem catalyst to enable the continuous generation of HNO from physiologically abundant glucose and L-arginine, and demonstrate that the integrated tandem catalyst can be used to create a long-lasting antithrombotic coating.

Results

The design of graphene–haemin–GOx tandem catalyst

Haemin, an iron porphyrin species, is the catalytic centre of nitric oxide synthase. Free haemin itself is generally inactive as a catalyst because it undergoes molecular aggregation and oxidative destruction under physiological conditions[35]. Resin-supported hydrophilic iron porphyrin derivatives have previously been shown to be active for the oxidation of L-arginine, but with a rather limited turnover number due to a rapid loss of catalytic activity[36]. This system is also not suitable for practical clinical applications because it requires a high concentration of H_2O_2 oxidant (38 mM), well beyond the physiological concentration. Recent studies have shown that monomeric haemin can be immobilized onto graphene to form a stable graphene–haemin conjugate that exhibits peroxidase-like activity for a variety of biomimetic oxidation reactions, using H_2O_2 as the oxidant[37,38].

To create the tandem catalyst, we immobilized monomeric haemin onto graphene through π–π interactions and covalently linked GOx with graphene to form a graphene–haemin–GOx conjugate (Fig. 1). With the integration of GOx in the conjugates, we expect to produce H_2O_2 locally from endogenous glucose for the subsequent haemin-catalysed oxidation of L-arginine to generate antithrombotic HNO species. In this way, this complex conjugate can be used as an effective biomimetic catalyst for the generation of HNO species using only endogenous species, namely, glucose and L-arginine. Importantly, the physiological concentrations of glucose, L-arginine and the required HNO levels for antiplatelet activity follow a nearly ideal cascade: blood glucose concentration is ca. 2–5 mM, capable of creating more than enough peroxide to oxidize L-arginine, which is present at ca. 200 μM. The amount of HNO necessary for significant antithrombotic effects is probably in the sub-μM range[32], which is at least three to four orders of magnitude lower than actual L-arginine concentrations.

Graphene–haemin for HNO production

The catalytic oxidation characteristics of graphene–haemin conjugates were initially investigated. Graphene was obtained by hydrazine reduction of exfoliated graphene oxide[9] prepared via Hummer's method[39]. The immobilization of monomeric haemin on graphene via π–π stacking was conducted using our previously reported approach[37]. L-arginine oxidation reactions were conducted by dispersing the graphene–haemin catalyst in a pH 7.4 PBS buffer with 200 μM L-arginine, along with 5 mM H_2O_2 as the oxidant (Fig. 2a). The L-arginine oxidation reaction could potentially result in multiple different products including NO or HNO. We have conducted extensive characterizations to demonstrate that the product is predominantly HNO. For product identification, the generated HNO dimerizes to form nitrous oxide over time, which is detectable by gas-phase Fourier transform infrared (FT-IR) spectroscopy[40]. The gas-phase FT-IR spectrum of the headspace gas of reaction vessel confirms the presence of nitrous oxide with two stretching bands at 2,211 and 2,235 cm^{-1} (Supplementary Fig. 1). The NO stretching bands at 1,790 and 1,810 cm^{-1} are not observed, excluding NO as the product of the reaction. The headspace gas is also tested by gas chromatography–mass spectrometry (GC-MS) for nitrous oxide detection[41], which further proves the existence of HNO (Supplementary Fig. 2). In addition, chemiluminescence

analysis, which can selectively detect p.p.b. levels of NO, but not HNO nor nitrous oxide, also demonstrates that there is no NO produced from the oxidation reaction (Supplementary Fig. 3). The expected by-product L-citrulline is also tested by LC-MS[42], further confirming the reaction pathway (Supplementary Fig. 4).

The above studies demonstrate that a graphene–haemin conjugate can function as an effective catalyst for the production of HNO. However, those methods are not capable of quantifying the generated HNO amount in reaction solution. Therefore, a fluorescence diaminofluorescein (DAF) assay was used. It has been documented that HNO can react with diaminofluorescein-2 to form diaminofluorescein-triazole with fluorescence emission[43]. The fluorescence spectrum was monitored at different time intervals (Fig. 2b), and the intensity increase of the emission peak at 515 nm was calibrated with the corresponding HNO concentrations (Fig. 2c). The DAF assay clearly shows the production of HNO immediately after the introduction of H_2O_2 to a graphene–haemin-catalysed reaction mixture, while the control reaction without the graphene–haemin conjugate does not yield any signal (Fig. 2c). Significantly, for the reactions with the equivalent amount of haemin, the graphene–haemin catalysts exhibit a remarkably higher activity, while the free haemin hardly shows any catalytic activity at all (Fig. 2c). Such a difference in catalytic behaviour can probably be attributed to the monomeric molecular structure of haemin on graphene supports. For free haemin, the active catalytic sites are limited because of molecular aggregation of haemin to form inactive dimers. The catalytic turnover frequency of graphene–haemin is calculated to be 0.015 min^{-1} (Fig. 2c), which greatly exceeds that of the previously reported resin-supported system (0.0016 min^{-1})[36]. Moreover, graphene–haemin conjugates also exhibit exceptional catalytic activity stability, with nearly a constant turnover rate over a 50-min test period, while the previously reported resin-supported haemin could only catalyse the reaction for about 6 min before a total loss of its catalytic activity[36].

Graphene–haemin–GOx for HNO production

Although, as demonstrated above, the graphene–haemin conjugates can effectively catalyse the oxidation of L-arginine to generate HNO, this reaction requires a relatively high concentration (~ 5 mM) of H_2O_2 oxidant that is far above the physiological H_2O_2 concentration (10^{-9}~10^{-7} M)[44]. To apply the graphene–haemin catalyst for practical applications under physiological conditions, a mechanism to locally produce desired levels of H_2O_2 is required. To this end, linking GOx to the graphene–haemin conjugates can offer an approach to elevate the local H_2O_2 concentration through the oxidation of blood glucose. GOx was anchored via a N-hydroxysuccinimide–ethyl(dimethylaminopropyl) carbodiimide (NHS–EDC) coupling reaction and linked to the edge and defect site carboxyl groups of graphene. NHS–EDC coupling has been successfully used for the covalent linkage of GOx onto graphene oxide previously[45]. Stained transmission electron microscopy shows dark features of around 10 nm size distributed around the edges or defective sites of graphene, which is attributed to the successful linkage of GOx (Supplementary Fig. 5). The formation of graphene–haemin–GOx is also supported by zeta potential measurements (Supplementary Table 1). Once the graphene–haemin–GOx conjugates were obtained, H_2O_2 production activity was tested in the presence of glucose and L-arginine (Supplementary Fig. 6), demonstrating that GOx retains good activity after chemical linkage onto the graphene.

The integrated catalysts were then used to catalyse the L-arginine oxidation reaction, and the HNO generation behaviour was studied using the DAF-based HNO assay. In pH 7.4 PBS buffer containing physiological concentrations of glucose (5 mM) and L-arginine (200 μM), the graphene–haemin–GOx conjugates produce HNO after a short activation stage (~5 min; Fig. 3a). This lag might be due to the necessary accumulation of an adequate H_2O_2 concentration at the surface of the graphene. For a series of control experiments, graphene–haemin–GOx catalysts in a solution of only glucose cannot produce any HNO, and a similar result was obtained for a solution containing only L-arginine, but not glucose (Fig. 3a). In a solution with both glucose and L-arginine, if only graphene–haemin conjugates or graphene–GOx conjugates alone are introduced, no HNO production is observed. Taken together, these findings clearly demonstrate that HNO production is observed only when the graphene–haemin–GOx conjugates, glucose and L-arginine are all present (Fig. 3a). The real-time reaction behaviour of this mixture was also monitored (Fig. 3b). Overall, the graphene–haemin–GOx conjugates can maintain good and stable activity over an extended period, and exhibits excellent recyclability (Fig. 3b).

Antithrombotic behaviour of graphene–haemin–GOx-embedded film

Our studies have clearly demonstrated that graphene–haemin–GOx conjugates can function as effective catalysts for the generation of HNO with endogenous components. To further investigate whether the graphene–haemin–GOx conjugates can offer an effective solution for potential biomedical applications, we embedded the conjugates (at ~40 wt%) in a commercially available polyurethane (Tecophilic® SP-93A-100) that was then spin coated to form biocompatible films. Control thin film samples were also prepared with embedded graphene, graphene–haemin or graphene–GOx (at the same wt%). All the films were then immersed into platelet-rich rabbit blood plasma for 3 days, and then examined by scanning electron microscopy to evaluate the platelet adhesion characteristics[46]. Control films containing graphene, graphene–haemin or graphene–GOx exhibited very rough surfaces after blood contact, indicating obvious adhesion of a significant number of blood platelets (Fig. 4a–c,e–g). In contrast, the film containing graphene–haemin–GOx shows a minimum morphology change before and after blood contact (Fig. 4d,h), clearly demonstrating excellent antiplatelet function.

Discussion

By simultaneously conjugating haemin and GOx on graphene, we have created an integrated tandem catalyst that can drive a reaction cascade to allow for *in situ* generation of H_2O_2 for the oxidation of L-arginine. This process can thus allow sustained generation of HNO from physiological glucose, L-arginine and blood oxygen. The embedment of such tandem catalysts into biocompatible films can create a surface coating with excellent antiplatelet characteristics, offering a potential solution to sustained generation of antithrombotic HNO species on medical devices when in contact with fresh blood. Overall, our studies demonstrate a general strategy to integrate molecular catalysts and enzymatic catalysts on the same platform for them to synergistically facilitate complex reaction pathways under mild physiological relevant conditions, and enable important chemical transformations not

otherwise readily possible. It can have an impact on diverse areas including biomedicine and green chemistry.

Methods

Preparation of graphene–haemin–GOx conjugates

The preparation of graphene–haemin–GOx conjugates are followed stepwise via immobilization of haemin on graphene surface, and then linkage of GOx to the carboxyl groups at the edge and defect site of graphene. The graphene–haemin conjugates were prepared using the previously reported protocols[37]. Graphene–haemin conjugates were then mixed with NHS–EDC coupling agent for 2 h, centrifuged and washed, followed by stirring with 0.1 mg ml $^{-1}$ GOx in pH 7.4 PBS buffer overnight for GOx linkage. Graphene–haemin–GOx conjugates were then centrifuged and washed with a pH 7.4 PBS buffer.

Characterization of L-arginine oxidation reaction

L-arginine oxidation reactions by graphene–haemin were carried out in the presence of 200 μM L-arginine and 5 mM H_2O_2 in a pH 7.4 PBS buffer. L-arginine oxidation reactions by graphene–haemin–GOx were carried out in the presence of 200 μM L-arginine and 5 mM glucose in a pH 7.4 PBS buffer. The product was characterized using FT-IR, GC-MS, DAF assay and chemiluminescence. For FT-IR spectroscopy, the gas-phase FT-IR spectrum of the headspace gas was taken after 2-h reaction. For GC-MS measurement, the headspace gas was injected into an Agilent 6890-5975 GC-MS with a 30 m Rt®-Q-Bound column (Resteck Co, Columbia, MD) at an operating oven temperature of 45 °C under 14.6 p.s.i. helium carrier gas. For the DAF assay, 10 μM DAF-2 was added to the reaction solution. The excitation wavelength was 448 nm. At each time interval, florescence spectra were obtained from an average of five accumulations. Peak intensities of 515 nm were also monitored continuously for reaction catalysed by graphene–haemin–GOx conjugates. For chemiluminescence, the solution after 2-h reaction was bubbled with Ar and the products were measured via a chemiluminescence NO Analyzer™, Model 280 (Sievers Instruments, Boulder, CO). *In situ* measurements were also carried out.

Antithrombotic film fabrication and antithrombotic studies

Tecophilic® SP-93A-100 polyurethane was dissolved in tetrahydrofuran to make a solution of 40 mg ml $^{-1}$. Graphene, graphene–haemin, graphene–GOx or graphene–haemin–GOx were then mixed with polymer solution and films cast on silicon substrates by spin coating. Films were peeled off after drying. Arterial blood from New Zealand white rabbits, weighing 2.5–3 kg, was drawn into a 9:1 volume of a blood:-anticoagulant citrate solution. The National Institutes of Health guidelines for the care and use of laboratory animals (NIH Publication number 85–23 Rev. 1985) were observed throughout. The citrated whole blood was centrifuged at 110*g* for 15 min at 22 °C. Platelet-rich plasma was collected from the supernatant. Films were first immersed in a pH 7.4 PBS buffer containing 200 μM L-arginine and 5 mM glucose for 30 min, and then immersed in platelet-rich plasma for 3 days. Films were then washed with pH 7.4 PBS buffer, dried and sputtered with gold for platelet aggregation and thrombus formation investigation by JEOL JSM-6700F FE-SEM.

Supplementary Material

Refer to Web version on PubMed Central for supplementary material.

Acknowledgments

Y.H. acknowledges support by the NIH Grant 1DP2OD007279, X.D. acknowledges support by the NIH Grant 1DP2OD004342-01 and M.E.M. acknowledges the support by the NIH Grant (EB-000783).

References

1. Fiedler D, Leung DH, Bergman RG, Raymond KN. Selective molecular recognition, C-H bond activation, and catalysis in nanoscale reaction vessels. Acc Chem Res. 2005; 38:349–358. [PubMed: 15835881]
2. Breslow R, Overman LE. 'Artificial enzyme' combining a metal catalytic group and a hydrophobic binding cavity. J Am Chem Soc. 1970; 92:1075–1077. [PubMed: 5451011]
3. Hailes HC, Dalby PA, Woodley JM. Integration of biocatalytic conversions into chemical syntheses. J Chem Technol Biotechnol. 2007; 82:1063–1066.
4. Marr AC, Liu S. Combining bio- and chemo-catalysis: from enzymes to cells, from petroleum to biomass. Trends Biotechnol. 2011; 29:199–204. [PubMed: 21324540]
5. Krumlinde P, Bogar K, Backvall JE. Asymmetric synthesis of bicyclic diol derivatives through metal and enzyme catalysis: application to the formal synthesis of sertraline. Chem Eur J. 2010; 16:4031–4036. [PubMed: 20196154]
6. Deska J, Ochoa CdP, Backvall J-E. Chemoenzymatic dynamic kinetic resolution of axially chiral allenes. Chem Eur J. 2010; 16:4447–4451. [PubMed: 20309981]
7. Wang ZJ, Clary KN, Bergman RG, Raymond KN, Toste FD. A supramolecular approach to combining enzymatic and transition metal catalysis. Nat Chem. 2013; 5:100–103. [PubMed: 23344446]
8. Stankovich S, et al. Synthesis of graphene-based nanosheets *via* chemical reduction of exfoliated graphite oxide. Carbon NY. 2007; 45:1558–1565.
9. Li D, Mueller MB, Gilje S, Kaner RB, Wallace GG. Processable aqueous dispersions of graphene nanosheets. Nat Nanotech. 2008; 3:101–105.
10. Tung VC, Allen MJ, Yang Y, Kaner RB. High-throughput solution processing of large-scale graphene. Nat Nanotech. 2009; 4:25–29.
11. Dai BY, et al. High-quality single-layer graphene *via* reparative reduction of graphene oxide. Nano Res. 2011; 4:434–439.
12. Tung VC, et al. Surfactant-free water-processable photoconductive all-carbon composite. J Am Chem Soc. 2011; 133:4940–4947. [PubMed: 21391674]
13. Feng H, et al. A low-temperature method to produce highly reduced graphene oxide. Nat Commun. 2013; 4:1539. [PubMed: 23443567]
14. Kuila T, et al. Chemical functionalization of graphene and its applications. Prog Mater Sci. 2012; 57:1061–1105.
15. Dwyer A. Surface-treated catheters-a review. Semin Dial. 2008; 21:542–546. [PubMed: 19000120]
16. Radomski MW, Palmer RMJ, Moncada S. The role of nitric-oxide and cGMP in platelet-adhesion to vascular endothelium. Biochem Biophys Res Commun. 1987; 148:1482–1489. [PubMed: 2825688]
17. Vaughn MW, Kuo L, Liao JC. Estimation of nitric oxide production and reaction rates in tissue by use of a mathematical model. Am J Physiol. 1998; 274:H2163–H2176. [PubMed: 9841542]
18. Keefer LK. Progress toward clinical application of the nitric oxide-releasing diazeniumdiolates. Annu Rev Pharmacol Toxicol. 2003; 43:585–607. [PubMed: 12415121]
19. Frost MC, Reynolds MM, Meyerhoff ME. Polymers incorporating nitric oxide releasing/generating substances for improved biocompatibility of blood-contactincy medical devices. Biomaterials. 2005; 26:1685–1693. [PubMed: 15576142]

20. Major TC, et al. The attenuation of platelet and monocyte activation in a rabbit model of extracorporeal circulation by a nitric oxide releasing polymer. Biomaterials. 2010; 31:2736–2745. [PubMed: 20042236]
21. Yan Q, Major TC, Bartlett RH, Meyerhoff ME. Intravascular glucose/lactate sensors prepared with nitric oxide releasing poly(lactide-co-glycolide)-based coatings for enhanced biocompatibility. Biosens Bioelectron. 2011; 26:4276–4282. [PubMed: 21592764]
22. Parzuchowski PG, Frost MC, Meyerhoff ME. Synthesis and characterization of polymethacrylate-based nitric oxide donors. J Am Chem Soc. 2002; 124:12182–12191. [PubMed: 12371858]
23. Kroencke KD, Suschek CV. Adulterated effects of nitric oxide -generating donors. J Invest Dermatol. 2008; 128:258–260. [PubMed: 18195740]
24. Hwang S, Meyerhoff ME. Polyurethane with tethered copper(II)-cyclen complex: preparation, characterization and catalytic generation of nitric oxide from S-nitrosothiols. Biomaterials. 2008; 29:2443–2452. [PubMed: 18314189]
25. Cha W, Meyerhoff ME. Catalytic generation of nitric oxide from S-nitrosothiols using immobilized organoselenium species. Biomaterials. 2007; 28:19–27. [PubMed: 16959311]
26. Giustarini D, Milzani A, Dalle-Donne I, Rossi R. Detection of S-nitrosothiols in biological fluids: a comparison among the most widely applied methodologies. J Chromatogr B Analyt Technol Biomed Life Sci. 2007; 851:124–139.
27. Mugesh G, du Mont WW, Sies H. Chemistry of biologically important synthetic organoselenium compounds. Chem Rev. 2001; 101:2125–2179. [PubMed: 11710243]
28. Cai W, Wu J, Xi C, Ashe AJ III, Meyerhoff ME. Carboxyl-ebselen-based layer-by-layer films as potential antithrombotic and antimicrobial coatings. Biomaterials. 2011; 32:7774–7784. [PubMed: 21794909]
29. Marletta MA. Nitric-oxide synthase—aspects concerning structure and catalysis. Cell. 1994; 78:927–930. [PubMed: 7522970]
30. Nathan C, Xie QW. Nitric-oxide synthases—roles, tolls, and controls. Cell. 1994; 78:915–918. [PubMed: 7522969]
31. Fukuto JM, Dutton AS, Houk KN. The chemistry and biology of nitroxyl (HNO): a chemically unique species with novel and important biological activity. Chem Bio Chem. 2005; 6:612–619.
32. Bermejo E, et al. Effect of nitroxyl on human platelets function. Thromb Haemost. 2005; 94:578–584. [PubMed: 16268475]
33. Pufahl RA, Wishnok JS, Marletta MA. Hydrogen peroxide-supported oxidation of N^G-hydroxy-L-arginine by nitric oxide synthases. Biochemistry. 1995; 34:1930–1941. [PubMed: 7531495]
34. Mukherjee M, Ray AR. Nitric oxide synthase-like activity of ion exchange resins modified with iron (III) porphyrins in the oxidation of L-arginine by H_2O_2: mechanistic insights. Catal Commun. 2007; 8:1431–1437.
35. Haber J, Mlodnicka T, Poltowicz J. Metal-dependent reactivity of some metalloporphyrins in oxidation with dioxygen. J Mol Catal. 1989; 54:451–461.
36. Mukherjee M, Ray AR. Biomimetic oxidation of L-arginine with hydrogen peroxide catalyzed by the resin-supported iron (III) porphyrin. J Mol Catal A Chem. 2007; 266:207–214.
37. Xue T, et al. Graphene-supported hemin as a highly active biomimetic oxidation catalyst. Angew Chem Int Ed. 2012; 51:3822–3825.
38. Guo Y, et al. Hemin-graphene hybrid nanosheets with intrinsic peroxidase-like activity for label-free colorimetric detection of single-nucleotide polymorphism. ACS Nano. 2011; 5:1282–1290. [PubMed: 21218851]
39. Hummers WS, Offeman RE. Preparation of graphitic oxide. J Am Chem Soc. 1958; 80:1339–1339.
40. Peng B, Meyerhoff ME. Reexamination of the direct electrochemical reduction of S-nitrosothiols. Electroanalysis. 2013; 25:914–921.
41. Donzelli S, et al. Generation of nitroxyl by heme protein-mediated peroxidation of hydroxylamine but not N-hydroxy-L-arginine. Free Radic Biol Med. 2008; 45:578–584. [PubMed: 18503778]
42. Kasper H, et al. Urinary amino acid analysis: a comparison of iTRAQ- LC-MS/MS, GC–MS, and amino acid analyzer. J Chromatogr B. 2009; 877:1838–1846.

43. Espey MG, Miranda KM, Thomas DD, Wink DA. Ingress and reactive chemistry of nitroxyl-derived species within human cells. Free Radic Biol Med. 2002; 33:827–834. [PubMed: 12208370]

44. Chance B, Sies H, Boveris A. Hydroperoxide metabolism in mammalian organs. Physiol Rev. 1979; 59:527–605. [PubMed: 37532]

45. Liu Y, Yu D, Zeng C, Miao Z, Dai L. Biocompatible graphene oxide-based glucose biosensors. Langmuir. 2010; 26:6158–6160. [PubMed: 20349968]

46. Wu Y, Zhou Z, Meyerhoff ME. *In vitro* platelet adhesion on polymeric surfaces with varying fluxes of continuous nitric oxide release. J Biomed Mater Res A. 2007; 81A:956–963. [PubMed: 17252544]

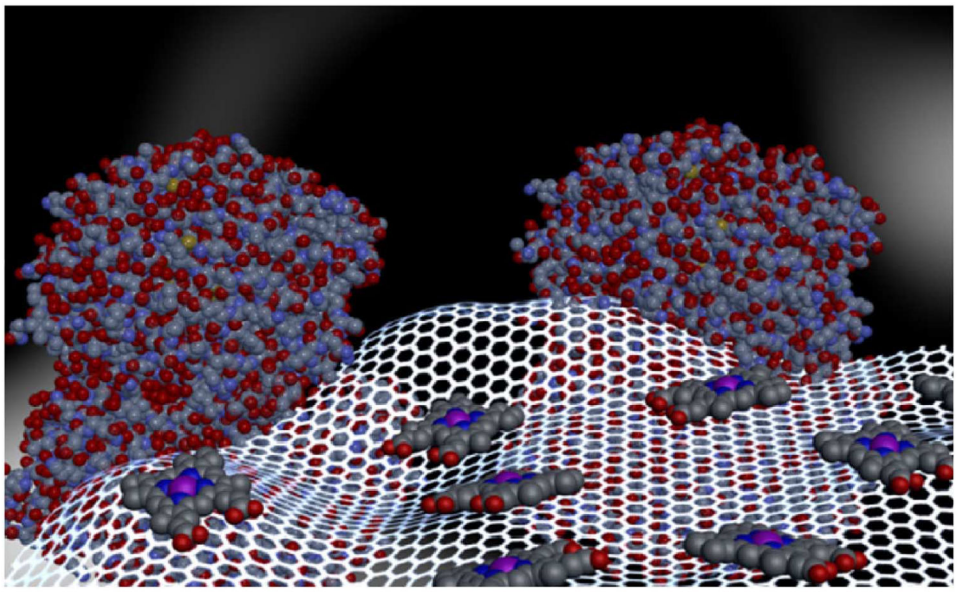

Figure 1. Schematic illustration of graphene–haemin–GOx conjugates

Monomeric haemin molecules are conjugated with graphene through π–π interactions to function as an effective catalyst for the oxidation of L-arginine, and GOx is covalently linked to graphene for oxidation of glucose and local generation of H_2O_2.

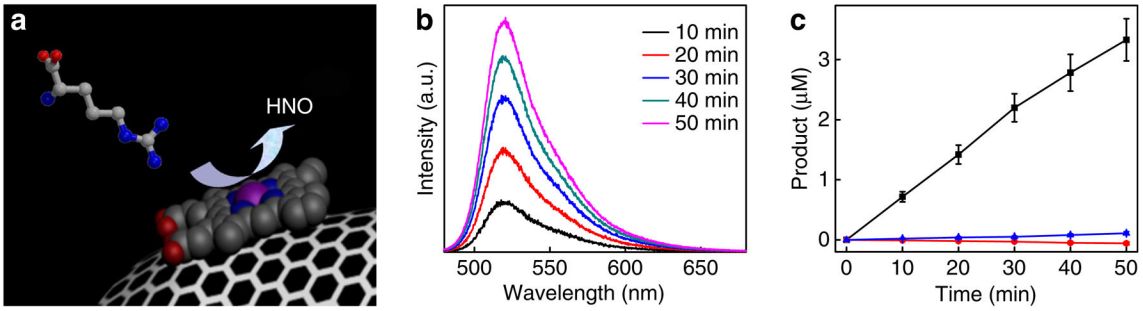

Figure 2. Graphene–haemin conjugate-catalysed oxidation of L-arginine

(**a**) A schematic illustration of graphene–haemin-catalysed L-arginine oxidation to produce HNO. (**b**) Relative fluorescence spectra at different reaction time obtained by DAF assay. (**c**) The HNO concentration determined by DAF assay. Black line represents product formation using graphene–haemin conjugate catalyst. Blue line represents product formation using free haemin catalyst. Red line represents product formation in a control experiment without catalyst. The size of the error bars represents the minimum to maximum values measured from at least three independent experiments.

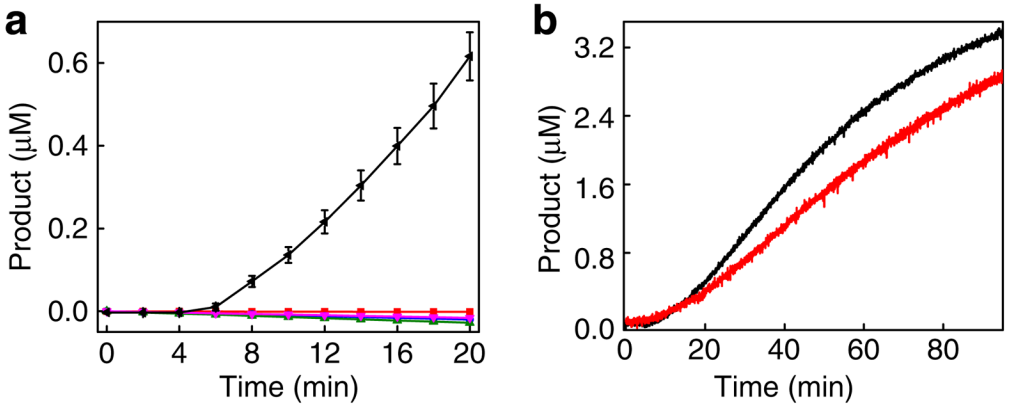

Figure 3. HNO generation catalysed by graphene–haemin–GOx conjugates

(**a**) Graphene–haemin–GOx catalysed HNO generation and control experiments. The production of HNO was quantified using a DAF assay. Black line, graphene–haemin–GOx in glucose and L-arginine; red line, graphene–haemin in glucose and L-arginine; blue line, graphene–GOx in glucose and L-arginine; green line, graphene–haemin–GOx in glucose; pink line, graphene–haemin–GOx in L-arginine. The size of the error bars represents the minimum to maximum values measured from at least three independent experiments. (**b**) Real-time HNO production catalysed by graphene–haemin–GOx (black line) and by the recycled graphene–haemin–GOx catalysts (red line).

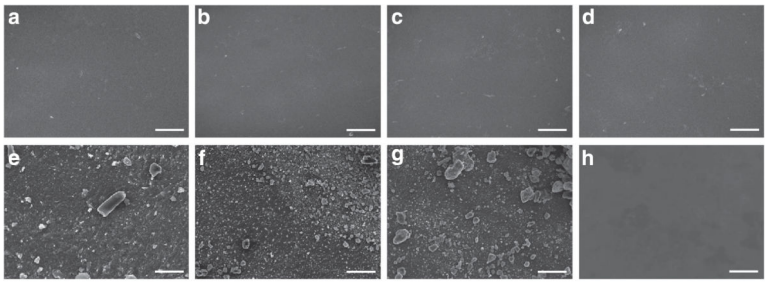

Figure 4. Antithrombotic behaviour of biocompatible films containing graphene–haemin–GOx conjugates

Scanning electron microscopic (SEM) images of as-formed films containing (**a**) graphene, (**b**) graphene–haemin, (**c**) graphene–GOx and (**d**) graphene–haemin–GOx; and the respective films after immersing into platelet-rich rabbit blood plasma for 3 days: (**e**) graphene, (**f**) graphene–haemin, (**g**) graphene–GOx and (**h**) graphene–haemin–GOx. Only films containing graphene–haemin–GOx exhibit a minimum morphology change by SEM after immersion into blood plasma compared to control films of graphene, graphene–haemin or graphene–GOx. Scale bars, 10 μm.